X-ray imaging of vortex cores in confined magnetic structures

Peter Fischer,[1,*] Mi-Young Im,[1] Shinya Kasai,[2] Keisuke Yamada,[3] Teruo Ono,[3] and André Thiaville[4]
[1] *Center for X-Ray Optics, Lawrence Berkeley National Laboratory, 1 Cyclotron Road, Berkeley, California 94720, USA*
[2] *Magnetic Materials Center, National Institute for Materials Science (NIMS), 1-2-1 Sengen, Tsukuba, Ibaraki, 305-0047 Japan*
[3] *Institute for Chemical Research, Kyoto University, Gokasyo, Uji 611-0011, Japan*
[4] *Laboratoire de Physique des Solides, Université Paris-sud, CNRS UMR 8502, Bâtiment 510, F-91405 Orsay Cedex, France*
(Received 11 February 2011; revised manuscript received 27 April 2011; published 15 June 2011)

Cores of magnetic vortices in micron-sized NiFe disk structures, with thicknesses between 150 and 50 nm, were imaged and analyzed by high-resolution magnetic soft x-ray microscopy. A decrease of the vortex-core radius was observed from approximately 38 to 18 nm with decreasing disk thickness. By comparing with full three-dimensional micromagnetic simulations showing the well-known barrel structure, we obtained excellent agreement, taking into account instrumental broadening and a small perpendicular anisotropy. The proven magnetic spatial resolution of better than 25 nm was sufficient to identify a negative dip close to the vortex core, originating from stray fields of the core. Magnetic vortex structures can serve as test objects for evaluating sensitivity and spatial resolution of advanced magnetic microscopy techniques.

DOI: 10.1103/PhysRevB.83.212402 PACS number(s): 75.70.Kw, 68.37.Yz, 75.78.Cd, 78.20.Ls

Magnetic vortex structures occur in soft ferromagnetic films and patterned elements, such as thin disks of the $Ni_{80}Fe_{20}$ alloy, as a result of the balance between exchange and dipolar energies. They are characterized by a curling magnetization in the plane of the disk with a vortex core in the center, where the magnetization points perpendicular to that plane. Two binary properties are commonly used to describe the vortex structure: the chirality, i.e., the counterclockwise or clockwise curling of the in-plane magnetization, and the polarity, i.e., the up or down direction of the vortex-core magnetization. The static[1–6] and dynamic[7–13] properties of these objects have recently attracted increased scientific interest, both for fundamental and applied reasons. For example, magnetic vortex structures were suggested as potential future high-density and nonvolatile recording systems,[14–17] since the size of the vortex core is proportional to the magnetic exchange length Λ, which can extend into the sub-10 nm regime,[18] and the magnetic core represents a very stable spin configuration, which is in fact protected by topology. However, to further advance the physical understanding of magnetic vortex structures, particularly the fast dynamics of the vortex core, through experimental investigations, advanced analytical microscopic tools with high spatial and temporal resolution are required. The first experimental images of magnetic vortex cores were obtained by magnetic force microscopy (MFM)[1] and, shortly after, the static internal structure of the vortex was studied at an almost atomic spatial resolution by spin-polarized scanning tunneling microscopy (SP-STM).[2] In addition, the ultrafast dynamics of the vortex structure was investigated by time-resolved Kerr microscopy,[19] revealing the rich spectrum of excitations and eigenmodes of the vortex.[20,21] Soft x-ray microscopies, which utilize circularly polarized x-rays to detect magnetic circular dichroism (XMCD) that provide an element-specific magnetic contrast,[22] have recently proven to be of great advantage in the study of the cores of magnetic vortices[23] and their dynamics, due to the simultaneously achievable combination of high spatial[24–26] and temporal resolution. Further, in order to assess the resolution of a magnetic microscopy technique, reliable magnetic test objects with a small, adjustable, and known size are indispensable. In this Brief Report, we quantitatively evaluate the use of a vortex core as such a test object by systematically comparing images obtained with state-of-the-art x-ray optics to three-dimensional (3D) micromagnetic simulations.

The experiments have been performed at the full-field soft x-ray microscope XM-1 located at beamline 6.1.2 at the Advanced Light Source (Berkeley, CA), where Fresnel zone plates provide a spatial resolution of better than 25 nm. Since XMCD probes the projection of the magnetic moments onto the photon propagation direction (z direction), in perpendicular geometry the M_z component of the vortex-core magnetization is directly imaged.[23] It appears as a dark or white contrast in the center of the disk, depending on whether the vortex core points in or out of the disk plane. Since the x-ray source at this instrument is a bending magnet, left and right polarization can be obtained by blocking the upper or lower half of the cone of the emitted x-rays. To suppress nonmagnetic background contributions and enhance magnetic contrast, two images, each with an illumination time of a few seconds, were recorded with left and right polarization and then divided by each other.

The samples were arrays of a few permalloy ($Ni_{80}Fe_{20}$, hereafter NiFe) disks, with a constant radius of 500 nm and varying thicknesses between 150 and 50 nm. The structures were defined by electron-beam lithography and subsequent electron-beam evaporation of NiFe onto 100-nm-thick Si_3N_4 membranes to allow for sufficient x-ray transmission. The vortex-core profiles were computed through 3D micromagnetic simulations using the public OOMMF code.[27] The mesh size was $4 \times 4 \times a$ nm^3 (with a close to 4 and adjusted with respect to the sample thickness), which is below the micromagnetic exchange length Λ in order to describe the core structure precisely,[28] and with a 3D meshing to describe the vortex-core structure along the sample thickness. From these 3D structures, radially averaged M_z profiles were evaluated at the surface of the disks, at a mid-thickness plane, and with thickness averaging.

The magnetic soft x-ray transmission microscopy (MTXM) images of an array of five dots, with 500 nm radius

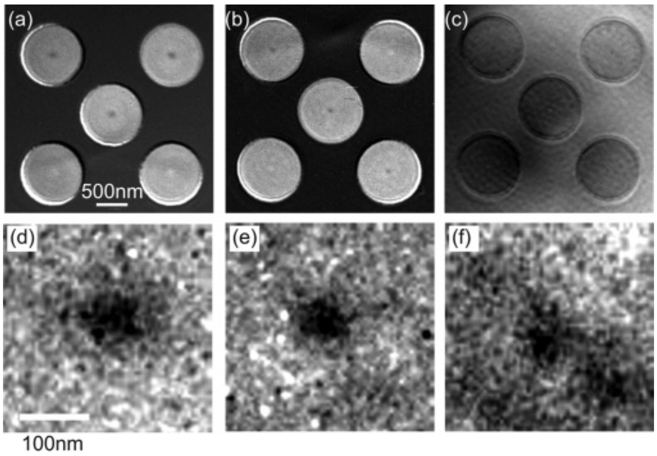

FIG. 1. Magnetic transmission soft x-ray microscopy images of permalloy disks with 500 nm radius and film thickness of (a) 150 nm, (b) 100 nm, and (c) 50 nm. The magnetic vortex cores can be identified by the black/white spots in the center, where the z component of the magnetization of the black vortex cores points into the paper plane and out for the white cores. Detailed views of some vortex cores, one for each thickness, are shown in (d)–(f).

and thicknesses of 50, 100, and 150 nm, are shown in Figs. 1(a)–1(c), respectively. While the in-plane curling magnetization does not show up in this perpendicular imaging geometry, the dark and white spots in the center of the dots, which represent the vortex cores, are clearly visible. Figures 1(d)–1(f) are a zoom into the center of some disks, i.e., the vortex core is displayed only. To analyze the M_z profile of the vortex, radially averaged intensity scans around the center of some individual dots are displayed in Figs. 2(a) and 2(c) (white cores), and 2(b) and 2(d) (black cores). Each radius step of 1 nm in the intensity scans is displayed by a single black dot. These profiles show a decrease of the vortex-core radius W (measured by the half width at half maximum size, HWHM) from approximately 38 to 18 nm, with decreasing disk thickness from 150 to 50 nm. Interestingly, with increasing thickness, a dip develops around the vortex core and the core intensity increases. The statistics on the five-dot groups in Fig. 1 also reveal some scatter in core intensity and dip amplitude. Dot-to-dot variations may be ascribed to illumination nonuniformities. The observed decrease of the signal-to-noise ratio for smaller sample thickness is a measure of the sensitivity of the technique.

Micromagnetic calculations were performed using the commonly assumed parameters for NiFe: spontaneous magnetization $M_s = 800$ kA/m and exchange constant $A = 13$ pJ/m, so that the exchange length reads $\Lambda = \sqrt{2A/(\mu_0 M_s^2)} = 5.7$ nm here. Whereas at zero thickness the analytical profile[29] is recovered, with $W = 1.13\Lambda$, as the thickness increases, the profiles adopt the "barrel" shape described by Hubert,[18] with a quasilinearly increasing width at the sample mid-plane and a slightly reduced width at the surfaces. The HWHM values for the vortex-core sizes W derived from that model are plotted in Fig. 3. Since only one characteristic length (exchange length Λ) is involved in this problem, Fig. 3 also shows the reduced values for the thicknesses h/Λ and W/Λ. As the transmitted signal in MTXM averages the magnetization along the sample thickness, which is complementary to surface sensitive techniques such as scanning tunneling microscopy (STM), we use the HWHM of the thickness-averaged intensity profiles in the following discussion.

These calculated profiles are superposed to the experimental data in Fig. 2 by the solid lines. In a first series of calculations [Figs. 2(a) and 2(b)], the NiFe was assumed to be perfectly soft, with no perpendicular anisotropy. Here, the dip of the opposite sign around the vortex core is extremely weak, and independent of the thickness. The physical origin of this ring of opposite perpendicular magnetization quantifies the response of the sample to the stray field from the core moment. In addition, it is found that the calculated core profile is narrower than in the experiments. In a second step, we included perpendicular anisotropy of $K = 10$ kJ/m^3 (corresponding to a moderate anisotropy field $\mu_0 H_K = 250$ G)[30] and we observed that the dip in the calculation be-

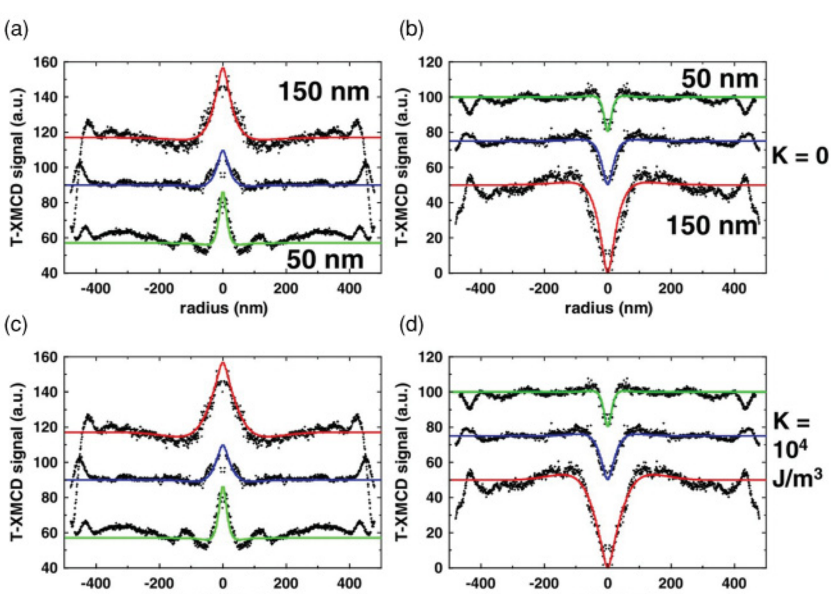

FIG. 2. (Color online) Radially averaged intensity profiles for individual (a), (c) white and (b), (d) black cores (radius step 0.2 pixel ≈ 1 nm) for the three sample thicknesses. The solid lines (red: 150 nm, blue: 100 nm, green: 50 nm) show the computed profiles for the thickness-averaged perpendicular magnetization, with a perpendicular anisotropy constant (a), (b) $K = 0$ kJ/m^3 and (c), (d) $K = 10$ kJ/m^3, and no instrumental broadening.

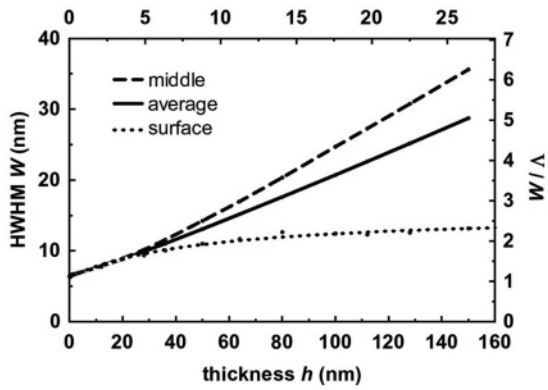

FIG. 3. HWHM values of the vortex-core width W as a function of sample thickness h, evaluated by micromagnetic calculations using the radial profiles of the perpendicular magnetization component at the sample surface, mid-plane, and for a thickness average. The perpendicular anisotropy is $K = 0$ kJ/m^3 and a negligible instrumental broadening is assumed ($\sigma = 1$ nm). The labels on the right and top axis give dimensions normalized to the exchange length Λ, which are the only relevant parameters for a zero anisotropy material when the disk diameter is much larger than the disk thickness.

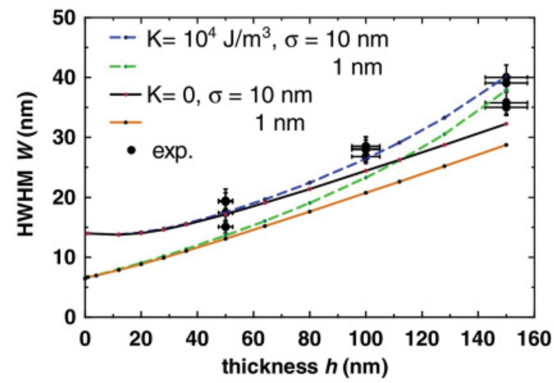

FIG. 4. (Color online) Comparison of vortex-core sizes as a function of sample thickness for various K values and instrumental broadening. Dots show the experimental values with error bars (5% in thickness from preparation uncertainties, and from the 95% confidence level of the core profile fits). Lines show the micromagnetic calculations based on the thickness-averaged profiles. The cases with perpendicular anisotropy $K = 0$ kJ/m^3 (solid lines) and $K = 10$ kJ/m^3 (dashed lines) are compared with, for each, a negligible instrumental broadening ($\sigma = 1$ nm) and the apparent value ($\sigma = 10$ nm).

comes more pronounced with increasing sample thickness. The existence of a perpendicular anisotropy in NiFe films has been proposed in order to interpret the appearance of so-called weak stripes at large thickness.[31] It is due to a nonzero magnetostriction combined with residual growth-induced film stress. The addition of this perpendicular anisotropy also leads to calculated core profiles that are in much better agreement with the x-ray experiments [see Figs. 2(c) and 2(d)], at least for the thicker films: for the two profiles at 150 nm thickness shown in Fig. 2, the regression coefficients computed on the 200 nm central disk are (a) 0.85 and (b) 0.86 without anisotropy, and increase to (c) 0.93 and (d) 0.95 with perpendicular anisotropy.

In order to be more systematic, a comparison of experimental and calculated core sizes is plotted in Fig. 4. The error bars in the experimental data are due to uncertainties in the thickness and to the noise level in the images. We note that the slope of core size versus thickness is not the same for experiments and $K = 0$ calculations. In this respect, we remark that changing the micromagnetic parameters will affect, in a similar proportion, the two axes (in the first approximation), therefore not mending this slope difference. One also observes that the perpendicular anisotropy increases the variation of core size with thickness. However, in order to account for the relatively larger core size at low thickness, it is necessary to introduce an instrumental broadening that expresses the spatial resolution of the microscope. As can be seen in Fig. 4, a very good agreement is obtained with a Gaussian broadening having the standard deviation $\sigma =$ 10 nm, corresponding to an instrumental Gaussian full width at half maximum (FWHM) of 23.2 nm, which is in full agreement with the nominal performance of the optics used in this experiment.

To conclude, we have performed a careful analysis of soft x-ray microscopy images of magnetic vortex cores in permalloy disks. Full 3D micromagnetic simulations have well reproduced the experimental data. Thus, vortex cores are suitable objects for quantifying the performance of advanced magnetic microscopy techniques. However, this requires a good knowledge of the sample parameters, including the perpendicular anisotropy. The decreasing core size with decreasing sample thickness challenges both the spatial resolution and the sensitivity of magnetic microscopy techniques, but this is the area of interest in terms of scientific and technological applications. Next-generation x-ray microscopies are indeed foreseeing Fresnel zone plate optics with a spatial resolution well below 10 nm.[32]

This work was supported by the Office of Science, Office of Basic Energy Sciences, Materials Sciences and Engineering Division, of the US Department of Energy.

*PJFischer@lbl.gov

[1] T. Shinjo, T. Okuno, R. Hassdorf, K. Shigeto, and T. Ono, Science **289**, 930 (2000).

[2] A. Wachowiak, J. Wiebe, M. Bode, O. Pietzsch, M. Morgenstern, and R. Wiesendanger, Science **298**, 577 (2002).

[3] J. Miltat and A. Thiaville, Science **298**, 555 (2002).

[4] C. Phatak, M. Tanase, A. K. Petford-Long, and M. DeGraef, Ultramicroscopy **109**, 264 (2009).

[5] J. Raabe, R. Pulwey, R. Sattler, T. Schweinbock, J. Zweck, and D. Weiss, J. Appl. Phys. **88**, 4437 (2000).

[6]J. K. Ha, R. Hertel, and J. Kirschner, Phys. Rev. B **67**, 224432 (2003).
[7]S. Choe, Y. Acremann, A. Scholl, A. Bauer, A. Doran, J. Stöhr, and H. A. Padmore, Science **304**, 420 (2004).
[8]J. Raabe, C. Quitmann, C. H. Back, F. Nolting, S. Johnson, and C. Buehler, Phys. Rev. Lett. **94**, 217204 (2005).
[9]K. Buchanan, P. Roy, M. Grimsditch, F. Fradin, K. Guslienko, S. Bader, and V. Novosad, Nature Phys. **1**, 172 (2005).
[10]S. Kasai, Y. Nakatani, K. Kobayashi, H. Kohno, and T. Ono, Phys. Rev. Lett. **97**, 107204 (2006).
[11]B. V. Waeyenberge *et al.*, Nature (London) **444**, 461 (2006).
[12]K. Yamada, S. Kasai, Y. Nakatani, K. Kobayashi, H. Kohno, A. Thiaville, and T. Ono, Nature Mater. **6**, 270 (2007).
[13]A. Vansteenkiste *et al.*, Nature Phys. **5**, 332 (2009).
[14]A. Drews, B. Krüger, G. Meier, S. Bohlens, L. Bocklage, T. Matsuyama, and M. Bolte, Appl. Phys. Lett. **94**, 062504 (2009).
[15]H. Jung, Y.-S. Yu, K.-S. Lee, S.-K. Kim, M.-Y. Im, P. Fischer, L. Bocklage, A. Vogel, M. Bolte, and G. Meier, Appl. Phys. Lett. **97**, 222502 (2010).
[16]M.-W. Yoo, K.-S. Lee, D.-E. Jeong, and S.-K. Kim, Phys. Rev. B **82**, 174437 (2010).
[17]Y.-S. Choi, J.-Y. Lee, M.-W. Yoo, K.-S. Lee, K. Y. Guslienko, and S.-K. Kim, Phys. Rev. B **80**, 012402 (2009).
[18]A. Hubert and R. Schäfer, *Magnetic Domains* (Springer, Berlin, 1998).
[19]J. P. Park, P. Eames, D. M. Engebretson, J. Berezovsky, and P. A. Crowell, Phys. Rev. B **67**, 020403 (2003).
[20]K. Y. Guslienko, B. A. Ivanov, V. Novosad, Y. Otani, H. Shima, and K. Fukamichi, J. Appl. Phys. **91**, 8037 (2002).
[21]K. Guslienko and V. Novosad, J. Appl. Phys. **96**, 4451 (2004).
[22]P. Fischer, D.-H. Kim, W. Chao, J. A. Liddle, E. H. Anderson, and D. T. Attwood, Mater. Today **9**, 26 (2006).
[23]K. W. Chou, A. Puzic, H. Stoll, D. Dolgos, G. Schütz, B. V. Waeyenberge, A. Vansteenkiste, T. Tyliszczak, G. Woltersdorf, and C. H. Back, Appl. Phys. Lett. **90**, 202505 (2007).
[24]W. Chao, B. H. Harteneck, J. A. Liddle, E. H. Anderson, and D. T. Attwood, Nature (London) **435**, 1210 (2005).
[25]W. Chao, J. Kim, S. Rekawa, P. Fischer, and E. Anderson, Opt. Express **17**, 17669 (2009).
[26]J. Vila-Comamala, K. Jefimovs, J. Raabe, T. Pilvi, R. Fink, M. Senoner, A. Maaßdorf, M. Ritala, and C. David, Ultramicroscopy **109**, 1360 (2009).
[27]M. Donahue and D. J. Porter, Tech. Rep., Interagency Report No. NISTIR 6376, 1999 (unpublished), see [http://math.nist.gov/oommf/oommf_cites.html] for reference to OOMMF.
[28]In the zero-thickness limit[29] that shows the smallest vortex-core size, the magnetization angle θ with the normal axis varies with radius r as $\theta = 1.19r/\Lambda$, which is close to the origin. As a result, for a mesh size $a = 4$ nm and $\Lambda = 5.7$ nm, the largest angle between neighboring cells would reach 46° (the core sitting between mesh points). Since the samples measured here are thicker, the largest angle between neighboring cells was in fact 27.5° (for the 50-nm-thick sample without perpendicular anisotropy and at the surfaces; this value falls to 5° for the 150-nm-thick sample with perpendicular anisotropy and at mid-thickness). This value is not very small, so that the vortex-core energy is not precisely evaluated,[33] giving rise to the well-known mesh friction effect when the core has to move. However, the cell-to-cell magnetization angle rapidly decreases away from the core center, so that the radial profile of the thickness-averaged magnetization is little affected (the considered HWHM core sizes are larger than $4a$), whereas some noise is visible in the calculated surface core widths in Fig. 3. Thus, for the smaller thicknesses calculated in Fig. 3, thinner meshes (down to $1 \times 1 \times 1$ nm^3) were used.
[29]E. Feldtkeller and H. Thomas, Phys. Condens. Mater. **4**, 8 (1965).
[30]F. Garcia *et al.*, Appl. Phys. Lett. **97**, 022501 (2010).
[31]J. Ben Youssef, N. Vukadinovic, D. Billet, and M. Labrune, Phys. Rev. B **69**, 174402 (2004).
[32]W. Chao (unpublished).
[33]A. Thiaville, J. M. García, R. Dittrich, J. Miltat, and T. Schrefl, Phys. Rev. B **67**, 094410 (2003).